Ultrafast transient reflectance of epitaxial semiconducting perovskite thin films

S. Y. Smolin,[1] M. D. Scafetta,[2] G. W. Guglietta,[1] J. B. Baxter,[1,a)] and S. J. May[2,a)]
[1]*Department of Chemical and Biological Engineering, Drexel University, Philadelphia, Pennsylvania 19104, USA*
[2]*Department of Materials Science and Engineering, Drexel University, Philadelphia, Pennsylvania 19104, USA*

(Received 7 June 2014; accepted 2 July 2014; published online 14 July 2014)

Ultrafast pump-probe transient reflectance (TR) spectroscopy was used to study carrier dynamics in an epitaxial perovskite oxide thin film of $LaFeO_3$ (LFO) with a thickness of 40 unit cells (16 nm) grown by molecular beam epitaxy on $(LaAlO_3)_{0.3}(Sr_2AlTaO_6)_{0.7}$ (LSAT). TR spectroscopy shows two negative transients in reflectance with local maxima at ~2.5 eV and ~3.5 eV which correspond to two optical transitions in LFO as determined by ellipsometry. The kinetics at these transients were best fit with an exponential decay model with fast (5–40 ps), medium (~200 ps), and slow (~ 3 ns) components that we attribute mainly to recombination of photoexcited carriers. Moreover, these reflectance transients did not completely decay within the observable time window, indicating that ~10% of photoexcited carriers exist for at least 3 ns. This work illustrates that TR spectroscopy can be performed on thin (<20 nm) epitaxial oxide films to provide a quantitative understanding of recombination lifetimes, which are important parameters for the potential utilization of perovskite films in photovoltaic and photocatalytic applications. © *2014 AIP Publishing LLC*.
[http://dx.doi.org/10.1063/1.4890241]

Perovskite oxides are a class of transition metal oxides with the chemical structure ABO_3. They have garnered much interest because of the diverse range of their physical and magnetic properties, including ferroelectricity, insulator-to-metal transitions, ferromagnetism, and superconductivity.[1] Many perovskite oxides exhibit band gaps in the visible range, leading to growing research interest in utilizing perovskite oxides for photovoltaic (PV) and photocatalytic (PC) applications.[2–9] However, understanding of the underlying ultrafast carrier dynamics in these materials is limited to a few studies,[10–12] despite the critical role that carrier lifetimes play in the design of materials for PV and PC applications.[13]

Here, we present a study of the carrier dynamics and recombination lifetimes in an epitaxial $LaFeO_3$ (LFO) thin film using ultrafast pump-probe spectroscopy. LFO is an interesting material system for PV and PC applications because its band gap is in the visible range (2.1–2.6 eV).[14,15] The relative chemical simplicity of LFO, compared to quaternary oxides, makes it an appealing system with which to begin investigations focused on identifying strategies to enhance carrier lifetimes in perovskites. Ultrafast spectroscopy is an ideal technique to study recombination lifetimes and has already been used for this purpose in other perovskite oxides.[10–12,16,17] Much of the previous work, however, was carried out on bulk crystals or polycrystalline films, as opposed to strained epitaxial thin films as reported here. The ability to measure carrier dynamics in ultrathin perovskites is a critical step in understanding how heterostructure-based approaches can be used to control lifetimes. To mitigate contributions from the substrate, the ultrafast pump-probe measurements were performed in a reflective geometry, using transient reflectance (TR) spectroscopy. The TR measurements of LFO reveal three distinct time regimes, which are primarily attributed to recombination of photoexcited carriers.

The epitaxial LFO thin film used in this study was deposited using molecular beam epitaxy with the La and Fe cations evaporated and sublimed, respectively, from pure elemental sources using standard effusion cells. The cation flux was calibrated using a quartz crystal monitor in conjunction with Rutherford backscattering spectroscopy (RBS) for relative cation concentration and x-ray reflectivity (XRR) for absolute atomic thickness determination. The film was deposited onto a $(LaAlO_3)_{0.3}(Sr_2AlTaO_6)_{0.7}$ (LSAT) (001) substrate (MTI Corp.) to a thickness of 40 unit cells. Prior to deposition, the substrate was heated to 200 °C, cleaned with isopropyl alcohol, and measured with ellipsometry to characterize optical properties. The film was grown at 625 °C in a chamber pressure of 5×10^{-7} Torr O_2 oxidizing gas. After deposition, the structural properties of the film were measured using X-ray diffraction (XRD) and XRR (Rigaku SmartLab). Static optical properties were measured using variable angle spectroscopic ellipsometry (J.A. Woolam M-2000U). More details about film growth and ellipsometric characterization are reported in Ref. 15.

High-resolution XRD measurements of the LFO film on LSAT substrate, shown in Figure 1, reveal a c-axis parameter of 3.981 Å, as obtained from the (002) pseudocubic reflection. This lattice constant is larger than bulk LFO (3.94 Å in pseudocubic notation)[18] and LSAT (3.87 Å), indicating that the substrate induces a compressively strained state in the film. The coherence length of the film, obtained from the FWHM of the (002) peak, is approximately equal to the film thickness, signifying that the film is crystalline and coherent throughout its thickness. The thickness fringes around the

a)Authors to whom correspondence should be addressed. Electronic addresses: jbaxter@drexel.edu and smay@coe.drexel.edu

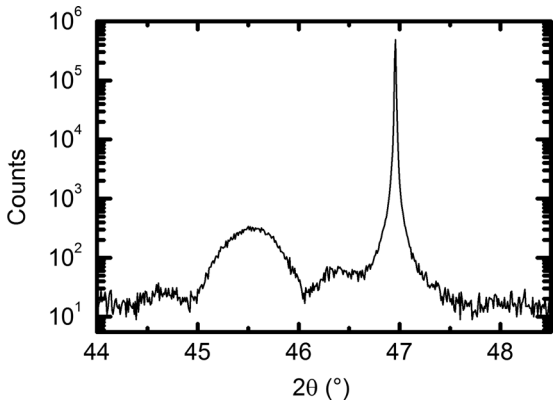

FIG. 1. X-ray diffraction obtained from the (002) peak of the LFO film on a LSAT substrate.

film peak indicate smooth interfaces. RBS was used to confirm that $LaFeO_3$ films grown under identical conditions have the correct nominal cation stoichiometry.

Carrier dynamics in LFO were studied with ultrafast TR spectroscopy. In this technique, an ultrafast optical pump pulse excites valence band electrons into the conduction band and, after a time delay, a weaker probe pulse monitors the reflectance of the sample. The time delay between the pump and probe was varied from 50 fs to 3 ns, giving information related to carrier dynamics on several time scales. The TR experiments were performed using an Ultrafast Systems (Helios) spectrometer and a regeneratively amplified Ti:sapphire laser (Coherent Libra HE). The laser outputs 50-fs pulses centered at 800 nm, with pulse energy of 3.5 mJ and a repetition rate of 1 kHz. A non-collinear optical parametric amplifier (OPA, Coherent OPerA Solo) was used to tune the pump energy to either 2.9 eV or 4.0 eV. The probe pulse was a white light continuum (1.8–3.8 eV) generated by focusing the 800 nm pulses onto a CaF_2 crystal and detected with a Si CCD array. Every other pump pulse was blocked with an optical chopper. The spectrometer measures the change in reflectance, $\Delta R(E,\,t) = \ln\left(\frac{I_{R,on}(E,t)}{I_{R,off}(E)}\right)$, where $I_{R,on}$ and $I_{R,off}$ are the intensities of probe light reflected by the sample with and without the pump pulse, respectively.

The intensity of light reflected by the samples is related to the refractive index of the sample, which is modulated by changes in free carrier density. Therefore, changes in free carrier densities can be observed by monitoring the ΔR signal.[19,20] Although there are several mechanisms for carrier-induced modification of the refractive index, the dominant contribution comes from bandfilling because this effect is roughly linearly proportional to carrier density.[19] Also known as the Burstein-Moss effect, bandfilling results in decreased absorption at energies equal to and slightly greater than the transition energy due to the filling of conduction or valence bands with electrons or holes, respectively. According to the Kramers-Kronig relationship, the decrease in absorption manifests itself as a decrease in the refractive index at and around the absorption edge,[19] which would appear as a negative ΔR signal at that position. In this work, the LFO film was pumped at either 2.9 eV or 4.0 eV, which is above the band gap of LFO but below the band gap of LSAT so that carriers are photoexcited in the film but not the substrate.

A characteristic 2D contour plot of the change in reflectance, $\Delta R(E,t)$, for the LFO film pumped at 4.0 eV is shown in Figure 2(a). The two key features are a negative reflectance transient at ~3.5 eV and a broad negative reflectance transient with a local maximum at ~2.5 eV. The positive reflectance features at ~2.7 and ~2.9 eV are due to the reflective nature of the measurement and are consistent with the bandfilling theory.[19] Ultrafast spectroscopic measurements performed in transmission geometry show similar negative transients, but the positive features are absent, as shown in supplementary material Figure S1.[21] Films photoexcited with 2.9 eV pump pulses instead of 4.0 eV pump pulses show very similar TR profiles, although the spectral region bounding the pump is obscured, as shown in Figure S2.

The spectral features can be observed more quantitatively using a spectral slice of the ΔR data at a specific pump-probe delay time, as shown in Figure 2(b) for a delay of 10 ps. The negative reflectance peaks at ~2.5 and ~3.5 eV correspond to the absorption onsets seen in the ellipsometry data, also shown in Figure 2(b), indicating that the features arise from optical transitions. The observation of two transitions matches other experimental and theoretical work on the electronic structure of LFO.[22] The LFO band gap of ~2.6 eV, determined by a Tauc plot of the ellipsometry data,[15] corresponds well to our transient peak at ~2.5 eV. Therefore, we attribute the bleach at ~2.5 eV to photoexcited electrons and holes with energies near the band edge and the recovery of this bleach to electron-hole recombination or trapping. The bleach feature at ~3.5 eV is attributed to a

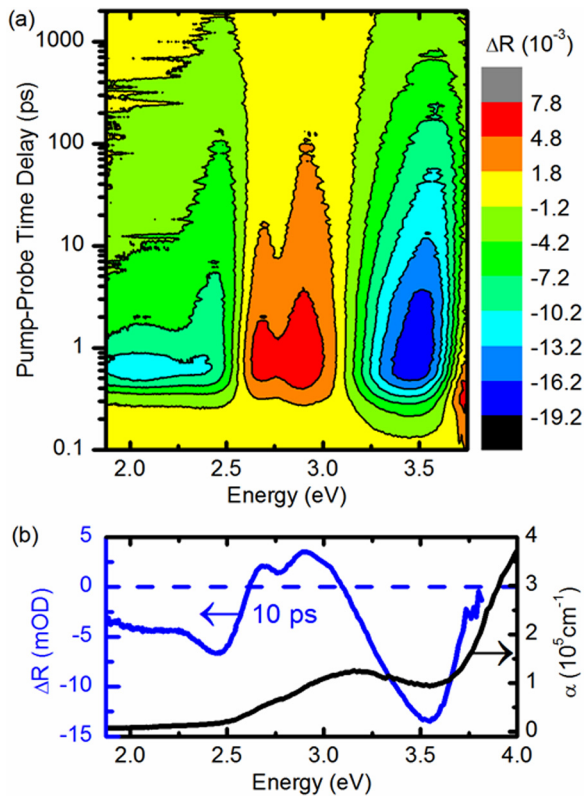

FIG. 2. (a) 2-D contour plot showing ΔR as a function of probe energy and pump-probe delay time. The pump energy was 4.0 eV at a power of 6.9 μJ/pulse. (b) A 1-D slice from the contour plot showing ΔR versus probe energy at a delay time of 10 ps, along with the absorption coefficient obtained from spectroscopic ellipsometry.

higher energy transition between a lower-lying valence band and the lowest conduction band or between the highest valence band and a higher-lying conduction band. Because electrons and holes must have the same recombination lifetime, if a fitted lifetime is similar at different probe energies of ~2.5 eV and ~3.5 eV, there is evidence that the fitted time constant represents recombination lifetime.[23,24]

Photoexcited carrier dynamics were studied by analyzing kinetics of the ~2.5 eV and ~3.5 eV reflectance transients. The kinetics were fit with a multi-exponential decay model convoluted with the instrument response

$$\frac{\Delta R}{|\Delta R_{\text{peak}}|} = \left[\sum_{i=1}^{n} A_i \exp\left(-\frac{t}{\tau_i}\right)\right] \otimes G_{IRF},$$

where $\frac{\Delta R}{|\Delta R_{\text{peak}}|}$ is the signal normalized by the peak magnitude of the signal and G_{IRF} is the Gaussian instrument response function. Kinetics at ~3.5 eV were fit with a three exponential model and the kinetics at ~2.5 eV required a four exponential model, where τ_1, τ_2, τ_3, and τ_{uf} correspond to the time constants of the fast (3–40 ps), medium (~200 ps), slow (~3 ns), and ultrafast (0.3–0.7 ps) part of the decay, respectively. The A_i parameters are the weights. Fewer exponential decay terms did not adequately fit the data, resulting in non-random residuals, as shown in Fig. S3. Because the spectral peaks shift slightly in energy with pump-probe delay time, fitting kinetics at a single energy introduces distortions into the kinetic trace. To mitigate these distortions, kinetics were monitored at the spectral peak instead of at a monochromatic energy. The fits of the two transients at ~2.5 eV and ~3.5 eV are shown in Figure 3. The model fits the data very well over three temporal orders of magnitude. The fitting parameters obtained for the different probe energies are given in supplementary material Tables SI and SII, and typical residuals for each probe energy are given in Figure S4.

Kinetics were measured at different pump fluences to further investigate the recombination mechanisms associated with different time scales. The power-dependence of normalized kinetic data and the fitted time constants at probe energies of ~2.5 eV and ~3.5 eV are shown in Figure 4. Pump power was varied between 0.9 and 11 μJ/pulse, with excitation at 2.9 eV. This range of power corresponds to photoexcited carrier densities of 0.6–7.2 $\times 10^{20}$ cm^{-3}, calculated using the absorption coefficient of 9×10^4 cm^{-1} determined by ellipsometry. Although these carrier densities are large, the peak ΔR signal remained linearly proportional to the pump power, Figure S5. In this high injection regime, recombination rates scale as n for Shockley-Read-Hall (SRH) recombination, n^2 for radiative recombination, and n^3 for Auger recombination.[25,26] Associated carrier lifetimes scale

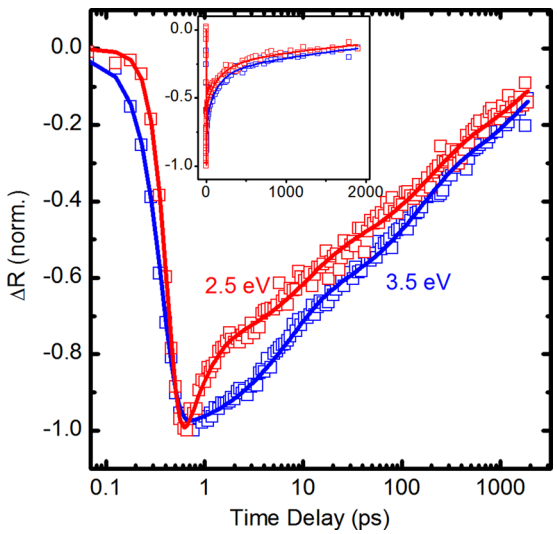

FIG. 3. TR kinetics for probe energies of ~3.5 eV and ~2.5 eV, with log and linear (inset) time axes, after photoexcitation at 4.0 eV with 6.9 μJ/pulse. Symbols are experimental data and lines are the fitted model.

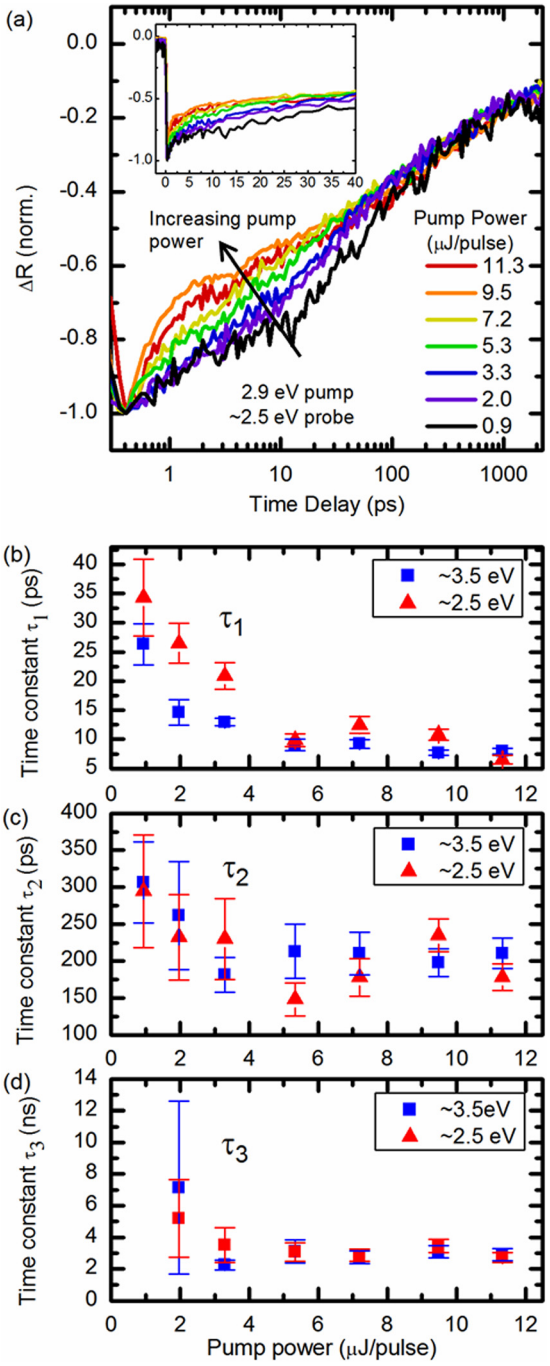

FIG. 4. (a) Normalized kinetic traces and (b)–(d) fitted time constants as a function of pump power. The pump energy is 2.9 eV and probe energies are indicated in each panel.

as n^0 for SRH recombination, n^{-1} for radiative recombination, and n^{-2} for Auger recombination.[26]

The ultrafast time constant τ_{uf} (0.3–0.7 ps) only appears in the reflectance transient at ~2.5 eV and is attributed to the cooling of hot photoexcited carriers via phonon interactions. Similar ultrafast relaxation was previously reported for $BiFeO_3$ (BFO).[9,11]

The fast time constant τ_1 (5–40 ps) was observed for both probe energies and decreases significantly with increasing pump power, Figure 4(a). This power dependence indicates that carrier-carrier interactions are important, as is the case with Auger and radiative recombination. The slight differences in time constants between the ~2.5 eV and ~3.5 eV probe energies indicate that interband scattering or trapping into mid-gap states may also contribute to the dynamics. Similar dynamics have been reported previously for BFO, although the underlying mechanism has not been conclusively identified. Yamada *et al.* found a fluence-dependent time constant between 0 and 200 ps in BFO thin films, which they attributed to Auger recombination.[12] In a BFO single crystal (220 μm thick), Sheu *et al.* assigned decays on ~10–50 ps scale to radiative recombination.[11] And in BFO polycrystalline films (150 nm), Jin *et al.* assigned dynamics on the order of tens of picoseconds to spin-phonon relaxation.[10] We do not expect spin-phonon relaxation to influence carrier dynamics in LFO, as a previous study of the magnetically similar BFO found no evidence of coupling between carrier dynamics and spin order.[11]

The medium time constant, τ_2, was on the order of ~200 ps for both probe energies, Figure 4(b), and is only weakly dependent on pump power. Moreover, good agreement between the fitted time constants at both probe energies over the entire range of pump power indicates that this represents a recombination process. Lifetimes independent of carrier density suggest that the time constant could represent either SRH or surface recombination. With a film thickness of only 16 nm, surface recombination may be significant because carriers have very short distances to diffuse to reach interfaces.

The longest time constant, τ_3, was on the order of 3 ns, Fig. 4(c), and is essentially independent of both pump power and probe energy. As with τ_2, SRH and surface recombination are consistent with the observed trends. Bleach recovery may also be attributed to trapping of carriers in localized states, as previously reported for BFO on nanosecond time scales.[12] Other reports in the literature have attributed nanosecond scale transients in BFO to a combination of lattice heating and radiative recombination.[11] They found significant changes in dynamics when varying pump energy because the excess energy resulted in changes in the lattice temperature. In our work, TR traces were similar for pump energies of 2.9 and 4.0 eV, as shown in Figure S6 and Table SIII, so we conclude that lattice heating does not significantly contribute to the observed dynamics. Regardless of the decay mechanisms, we note that more than 10% of photoexcited carriers remain for longer than 3 ns.

In conclusion, this work demonstrates that ultrafast TR measurements can be performed on epitaxially strained crystalline thin films of perovskite oxides with a thickness of less than 20 nm. The ultrafast reflectance transients at ~2.5 eV and ~3.5 eV correspond to the absorption spectrum of the LFO film. Kinetics at those transients were fit well by a multi-exponential decay model with fast (5–40 ps), medium (~200 ps), and long (~3 ns) time constants that we assign primarily to recombination of photoexcited carriers. By establishing the approach of using TR to quantify carrier dynamics, this work will enable future studies that can quantitatively probe the effects of strain, thickness, and the presence of interfaces on carrier lifetimes and recombination mechanisms in epitaxial perovskite films. The ability to use these strategies accessible in oxide heterostructures to engineer ultrafast carrier dynamics in perovskites films may provide promising means for enhancing their applicability as photovoltaic and photocatalytic materials.

This work was supported by the National Science Foundation through award ECCS-1201957. M.D.S. acknowledges support from the Department of Education (GAANN-RETAIN, Award No. P200A100117). The ultrafast spectrometer was acquired with funds from NSF MRI award DMR-0922929. X-ray diffraction was performed using the Centralized Research Facilities of the College of Engineering at Drexel University. The x-ray diffractometer was acquired with funds from NSF MRI award DMR-1040166. We thank Boris Yakshinskiy for RBS measurements at the Rutgers University Laboratory for Surface Modification.

[1]M. A. Peña and J. L. G. Fierro, Chem. Rev. **101**, 1981 (2001).
[2]B. A. Apgar, S. K. Lee, L. E. Schroeder, and L. W. Martin, Adv. Mater. **25**, 6201 (2013).
[3]J. W. Liu, G. Chen, Z. H. Li, and Z. G. Zhang, J. Solid State Chem. **179**, 3704 (2006).
[4]I. E. Castelli, T. Olsen, S. Datta, D. D. Landis, S. Dahl, K. S. Thygesen, and K. W. Jacobsen, Energy Environ. Sci. **5**, 5814 (2012).
[5]S. Y. Yang, J. Seidel, S. J. Byrnes, P. Shafer, C. H. Yang, M. D. Rossell, P. Yu, Y. H. Chu, J. F. Scott, J. W. Ager, L. W. Martin, and R. Ramesh, Nat. Nanotechnol. **5**, 143 (2010).
[6]I. Grinberg, D. V. West, M. Torres, G. Y. Gou, D. M. Stein, L. Y. Wu, G. N. Chen, E. M. Gallo, A. R. Akbashev, P. K. Davies, J. E. Spanier, and A. M. Rappe, Nature **503**, 509 (2013).
[7]E. Assmann, P. Blaha, R. Laskowski, K. Held, S. Okamoto, and G. Sangiovanni, Phys. Rev. Lett. **110**, 078701 (2013).
[8]P. V. Sushko, L. Qiao, M. Bowden, T. Varga, G. J. Exarhos, F. K. Urban, D. Barton, and S. A. Chambers, Phys. Rev. Lett. **110**, 077401 (2013).
[9]D. Schick, M. Herzog, H. Wen, P. Chen, C. Adamo, P. Gaal, D. G. Schlom, P. G. Evans, Y. Li, and M. Bargheer, Phys. Rev. Lett. **112**, 097602 (2014).
[10]Z. Jin, Y. Xu, Z. Zhang, G. Li, X. Lin, G. Ma, Z. Cheng, and X. Wang, Appl. Phys. Lett. **100**, 071105 (2012).
[11]Y. M. Sheu, S. A. Trugman, Y. S. Park, S. Lee, H. T. Yi, S. W. Cheong, Q. X. Jia, A. J. Taylor, and R. P. Prasankumar, Appl. Phys. Lett. **100**, 242904 (2012).
[12]Y. Yamada, T. Nakamura, S. Yasui, H. Funakubo, and Y. Kanemitsu, Phys. Rev. B **89**, 035133 (2014).
[13]J. B. Baxter, C. Richter, and C. A. Schmuttenmaer, Annu. Rev. Phys. Chem. **65**, 423 (2014).
[14]T. Arima, Y. Tokura, and J. B. Torrance, Phys. Rev. B **48**, 17006 (1993).
[15]M. D. Scafetta, Y. J. Xie, M. Torres, J. E. Spanier, and S. J. May, Appl. Phys. Lett. **102**, 081904 (2013).
[16]J. Bielecki, R. Rauer, E. Zanghellini, R. Gunnarsson, K. Dörr, and L. Börjesson, Phys. Rev. B **81**, 064434 (2010).
[17]Y. Yamada, H. K. Sato, Y. Hikita, H. Y. Hwang, and Y. Kanemitsu, Phys. Rev. Lett. **111**, 047403 (2013).
[18]H. Falcón, A. E. Goeta, G. Punte, and R. E. Carbonio, J. Solid State Chem. **133**, 379 (1997).
[19]B. R. Bennett, R. A. Soref, and J. A. del Alamo, IEEE J. Quantum Electron. **26**, 113 (1990).

[20]A. Othonos, H. M. van Driel, J. F. Young, and J. M. Baribeau, Solid State Commun. **82**, 325 (1992).
[21]See supplementary material at http://dx.doi.org/10.1063/1.4890241 for additional information regarding the transient reflectance data and fits.
[22]H. Wadati, D. Kobayashi, H. Kumigashira, K. Okazaki, T. Mizokawa, A. Fujimori, K. Horiba, M. Oshima, N. Hamada, M. Lippmaa, M. Kawasaki, and H. Koinuma, Phys. Rev. B **71**, 035108 (2005).
[23]Z. Huang, Y. Lin, X. Xiang, W. Rodriguez-Cordoba, K. J. McDonald, K. S. Hagen, K.-S. Choi, B. S. Brunschwig, D. G. Musaev, C. L. Hill, D. Wang, and T. Lian, Energy Environ. Sci. **5**, 8923 (2012).
[24]A. G. Joly, J. R. Williams, S. A. Chambers, G. Xiong, W. P. Hess, and D. M. Laman, J. Appl. Phys. **99**, 053521 (2006).
[25]J. L. Gray, in *Handbook of Photovoltaic Science and Engineering*, edited by A. Luque and S. Hegedus (John Wiley & Sons, West Sussex, UK, 2011), p. 94.
[26]J. Nelson, in *The Physics of Solar Cells* (Imperial College Press, London, UK, 2003), p. 99.